

BALÁZS LEMMER¹, ZOLTÁN JÁKÓI¹, NIKOLETT GULYÁS¹, SZABOLCS KERTÉSZ¹,
SÁNDOR BESZÉDES¹, ZSUZSANNA LÁSZLÓ¹, CECILIA HODÚR¹

THE EFFECT OF SONICATION AND STIRRING ON ULTRAFILTRATION OF FERMENTATION BROTH

Membrane separation is a widely used technique whose main obstacle is membrane fouling, during which a solution or particles accumulate on the membrane surface or inside its pores. This phenomenon causes both reversible and irreversible flow resistances that can be minimized with complementary techniques such as sonication and/or stirring. The application of ultrasonic energy can increase the flux by breaking the concentration polarization and cake layer on the membrane surface without affecting the intrinsic permeability of the membrane. Our work focused on cellulase and β -glucosidase enzyme recovery through sonicated/stirred ultrafiltration from the real fermentation broth, at which the fermentation liquid was produced from tobacco plants. Membrane filtrations were carried out in a laboratory-grade batch ultrafiltration cell, extended with stirrer and ultrasound processor. The effects of stirring speed and ultrasound treatment were investigated on the membrane's permeate flux efficiency and on the quality of recycled enzymes. Resistance values were calculated by the resistance-in-series model, as well as by Hermia's analysis, to reveal deeper, process-related information. Our results revealed that enzymes could be efficiently separated from real fermentation broth. Furthermore, the enzyme activity test showed that neither stirred nor sonicated processes were detrimental to the enzyme activity.

1. INTRODUCTION

The economically exploitable classic fossil energy sources on Earth are considerably limited. Biomass energy is one possible substitute, of which, for instance, bioethanol could be produced from numerous raw materials besides starches and sugars such as from lignocellulose sources [1]. However, lignocellulosic-based bioethanol production needs significant enzyme utilization. Enzymatic hydrolysis of a cellulosic matrix is a very cost-intensive processing step that is largely determined by the market price of

¹Department of Process Engineering, Faculty of Engineering, University of Szeged, 9 Moszkvai krt., Szeged, H6725, Hungary, corresponding author C. Hodúr, e-mail address: hodur@mk.u-szeged.hu

enzymes [2]. To reduce costs, our study focused on the membrane separation techniques, which are considered to be the most efficient methods for enzyme recovery [3], as they are widely used in special installations such as in bioreactors [4]. The fouling problem is one of the most important questions for the membrane application [5]. Both sonication and stirring were investigated as enhancements to the processing efficiency. Both methods should increase the permeation flux and reduce flow resistances which should make enzyme filtration cheaper and provide a more environmentally friendly processing method. The enhancing effect of stirring is well known due to the resulting increase in turbulence on the membrane surface.

Ultrasound (US) refers to sound waves with a frequency higher than 20 kHz, which, when passed through a medium, generates acoustic cavitation and induces surface vibrations. The phenomenon of mechanical vibrations is used to clean or disrupt membrane fouling and minimizes cake formation during filtration [6]. A supposed mechanical effect from the US are mechanical shear forces created by microstreaming and shock [7, 8]. Since our work is focused on enzyme recovery, it is important to know the effect of the US on not only the permeate flux but also on the enzymatic activity. Authors working with the US to achieve enzymatic hydrolysis have attributed the process to two different effects: i) temperature-induced acceleration [9], and ii) pressure-induced degradation [10]. The activity change in enzymes results predominantly from the variations of their secondary and tertiary chemical structures, while still controversial attributions are the different US frequencies, intensities and application conditions. In short, low-frequency US (<100 kHz) mainly promotes inhibition of enzymatic activity, which is probably caused by cavitation and shear forces [11]. Higher US frequencies should be applied to investigate their influence, which could be very different from that observed in low-frequency US [12].

2. MATERIALS AND METHODS

Membrane separations. Membrane separation was carried out with a laboratory-grade, stirred-batch, ultrafiltration cell with a capacity of 400 cm³ (Fig. 1). The cell was equipped with a polyethersulphone membrane 76 mm, in diameter, with a 10 kDa cut-off value (Sterlitech PW UF Membrane). During filtration, the samples – originated from the fermentation broth – were stirred and/or sonicated at the following combinations: without stirring and the US, only stirring, only US and both stirring and US. Stirring was carried out with a magnetic stirrer at a revolution range of 0–500 rpm and a 30 kHz ultrasound processor (Hielscher, UP100H with MS10 transducer). Sonication was used at 60% amplitude, half duty cycle and with a 30 mm membrane-transducer distance. Initially, the volume of the filtrated media was 200 cm³ (i.e., at the beginning of the ultrafiltration) which then has been reduced to 50 cm³, thus, gaining 150 cm³ of permeate. The transmembrane pressure between the two sides of the membrane was

0.3 MPa. The permeate was discharged continuously and fermentation broth was concentrated during the process.



Fig. 1. Sonicated ultrafiltration cell module during operation

The filtration time and permeate volume were measured. The membrane permeability J , $\text{dm}^3/(\text{m}^2 \cdot \text{h})$, is expressed as the permeate flux through the membrane:

$$J = \frac{dV}{Ad\tau} \quad (1)$$

where A is the filter's surface area, m^2 , V is the filtration volume, dm^3 , and τ is the filtration time, h. The total flow resistance, $1/\text{m}$, R_t consists of three components. One of them is the membrane resistance R_m , and the two other constitute the irreversible resistance R_{irr} and the reversible resistance R_{rev} :

$$R_t = R_m + R_{irr} + R_{rev} \quad (2)$$

The total flow resistance R , $1/\text{m}$, is:

$$R = \frac{dP}{\eta J} \quad (3)$$

where dP is the transmembrane pressure, Pa, η is the dynamic viscosity of the permeate, $\text{Pa} \cdot \text{s}$.

R_l was calculated by assuming the critical flux of separation, R_m was calculated from the flux of distilled water through a new and clean membrane, while R_{irr} was figured out from the flux of distilled water through a rinsed membrane after the separation [13]:

$$R_m = \frac{dp}{J_w \eta_w} \quad (4)$$

$$R_{irr} = \frac{dp}{J_{wA} \eta_w} - R_m \quad (5)$$

$$R_{rev} = \frac{dp}{J_C \eta_p} - R_{irr} - R_m \quad (6)$$

where J_w is the water flux of the clean membrane, $\text{dm}^3/(\text{m}^2 \cdot \text{h})$, η_w is the dynamic viscosity of water, $\text{Pa} \cdot \text{s}$, j_{wA} is the water flux after the concentration test, J_C is the constant flux at the end of the filtration, and η_p is the dynamic viscosity of the permeate.

The fermentation broth was obtained from the hydrolysis of experimental tobacco plants by cellulase sources from *Trichoderma reesei* (C2730, Sigma-Aldrich) and β -glucosidase from *Aspergillus niger* (Novozyme 188, Sigma-Aldrich) in equal volumes. The total enzyme concentration of the broth was 0.6 vol. %. C2730 cellulase (with a nominal enzyme activity of 700 U/g), containing β -glucanase units, catalyzes the breakdown of cellulose into glucose and cellobiose (and with significantly lower probability into higher glucose polymers), while β -glucosidase (with a nominal enzyme activity of 250 U/g) catalyzes the hydrolysis of cellobiose units into glucose molecules. C2730 enzyme protein has an average molecular mass of 85 kDa (which corresponds to approximately 0.09 μm in size), and the MW of the applied β -glucosidase is 26 kDa (approximately 0.03 μm), according to the datasheet provided by Sigma Aldrich. Cellobiose units (i.e., two β -D-glucose units linked by a $\beta(1-4)$ bond) have an average molecular size of 1.03 nm, whilst glucose molecules in an open-chain form (i.e., when dissolved in water) have an average length of 1.5 nm. The molecular size (weight) of a cellulose chain can vary greatly, depending on how many glucose units it contains, that is, which part of a given plant it has been extracted from. Therefore, the average particle size distribution of the ultrafiltrated fermentation media extended from 1 to 90 nm, since it contained the enzymes and the end products (i.e., saccharides) of the enzymatic digestion processes to the largest degree. Even so, it should definitely be taken into account that the fermentation broths might have contained larger particles as well, for example, higher carbohydrate polymers, contaminants or plant-originated proteins, but their average concentration compared to the enzymes and sugars discussed above, can be considered negligible.

The broth was centrifuged at 5400 rpm for 30 min and the supernatant was used for the separation. The supernatant had 1.9 ± 0.05 wt. % of dry matter and $\text{pH} = 5.5$. The

solid matter consisted of mono- and disaccharides from the hydrolysis of cellulose, small particles from the raw material, enzymes and other proteins.

Enhancement factor. Enhancement factor, E , is used to measure the permeate flux improvement [14]:

$$E = \frac{J_{\text{treated}}}{J_{\text{untreated}}} \quad (7)$$

where J_{treated} is the steady-state flux achieved when sonication and/or stirring was applied, and $J_{\text{untreated}}$ is the steady-state flux when neither stirring nor sonication was used.

Energy consumption. Power consumed by the stirrer (P_{str}) was calculated from [15]:

$$P_{\text{str}} = N_e d^5 n^3 \rho \quad (8)$$

$$N_e = k Re^m \quad (9)$$

$$Re = \frac{d^2 N \rho}{\eta} \quad (10)$$

where N_e is the power number, Re the Reynolds number. The constants k and m of eq. (9) were calculated after [16] since a paddle-type stirrer was used, d is the diameter of the stirrer, m , N is the stirring speed, 1/s, ρ is the density of the fluid, kg/m³, η is the viscosity.

Ultrasonic power dissipated in the liquid (P_{US}) was calculated by the calorimetric method [17] based on the measurement of the temperature increase due to the conversion of US energy into heat:

$$P_{\text{US}} = mc_p \frac{dt}{d\tau} \quad (11)$$

where m is the weight of the liquid, kg, c_p the specific heat capacity, J/(kg·K), and t is the temperature, K, τ is the time, s.

Hermia's empirical models. The Hermia model, one of the most comprehensive fouling prediction models, incorporates four different fouling mechanisms, namely: complete blocking, intermediate blocking, standard blocking and cake layer formation [18]. Four empirical models for dead-end filtration were developed by Hermia [19]. Equation (7) is based on constant pressure filtration laws that correspond to four basic types of fouling: complete blocking, intermediate blocking, standard blocking, and cake

layer formation. The considered type of fouling depends on the value of parameter n in the following equation:

$$\frac{d^2\tau}{dV^2} = K \left(\frac{d\tau}{dV} \right)^n \quad (12)$$

Here, V is the accumulated permeate volume, m^3 , K is the model constant, and n is the model parameter which depends upon the predominate fouling mechanism involved. Typical values of the parameter n are as follows: $n = 2$ – complete blocking, $n = 1$ – intermediate blocking, $n = 3/2$ – standard blocking and $n = 0$ if a gel layer is formed.

Hermia empirical model applicable to dead-end filtration was modified [20] for crossflow filtration:

$$\frac{dJ_p}{d\tau} = K_{CF} (J_p - J_{pss}) J_p^{2-n} \quad (13)$$

where J_p is the permeate flux, K_{CF} is the phenomenological coefficient dependent upon the specific fouling mechanisms, and J_{pss} is the steady-state permeate flux, m/s .

Enzyme activity. The enzyme activity was determined by the classical filter paper test. In laboratory fermenters with a volume of 100 cm^3 , 90 cm^3 of distilled water and 10 cm^3 of concentrated broths from ultrafiltration were added to 1 g of crystalline cellulose. Then the samples were incubated in a laboratory water bath heated to a constant temperature of $45 \text{ }^\circ\text{C}$. Every 2 h, 1 cm^3 of the sample was removed from the broth and boiled for 2 min to quench further enzyme activity. pH was then fixed at 5 by means of dilute H_2SO_4 and NaOH solutions.

The reducing sugar content, proportional to the enzyme activity, was determined spectrophotometrically by the 3,5-dinitrosalicylic acid (DNSA) method, at which 1 cm^3 of DNSA and 0.1 cm^3 of the sample were mixed and heated at $90 \text{ }^\circ\text{C}$ for 15 min. After cooling in ice water, 1 cm^3 of distilled water and 1 cm^3 of 40% potassium sodium tartrate were added to the samples. The absorbance was measured at 575 nm.

3. RESULTS

During the first series of experiments, the fermentation liquid was being ultrafiltrated without the application of ultrasound with different stirring speeds to determine the effects of it on the permeate flux. Figure 2 shows the results obtained for the change of flux under various stirring speeds. As shown in Fig. 2, the flux value of 0 rpm no US (no stirring, no sonication) was the lowest. Stirring creates higher flux at all stirring speeds, but over 300 rpm no significant flux increments could be observed. Every flux

curve starts from a similar and higher value followed by a rapid drop and an approximately steady-state period from 750 s. The decrease was observed at 0 rpm no US, and the increase of the stirring pH reduces the flux decrease.

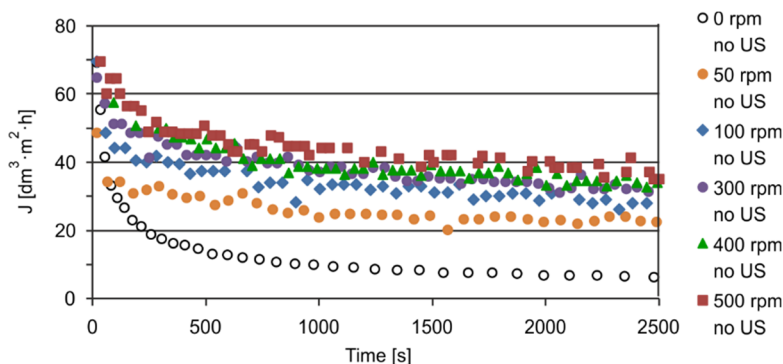


Fig. 2. Permeate flux of fermentation broth vs. time at different stirring speeds (no US means ultrasound was not used)

To characterize the flux, power functions with decreasing exponent values were fitted to each curve. The dynamics of the decrease is expressed by the index of fitted functions shown in Table 1, which presents the values of the fitted parameters and the degree of model fitness (represented by R^2 values).

Table 1

Fitted parameters of power functions

Parameter	0 rpm no US	50 rpm no US	100 rpm no US	300 rpm no US	400 rpm no US	500 rpm no US
Index	-0.493	-0.147	-0.169	-0.159	-0.173	-0.149
Intersection	8×10^{-5}	2×10^{-5}	3×10^{-5}	3×10^{-5}	4×10^{-5}	3×10^{-5}
R^2	0.999	0.919	0.9157	0.9299	0.9037	0.8569

That means that the character of the flux curves, i.e., the filtration mechanisms, were independent of the stirring speed. The intersection of the ordinate is also shown in Table 1. This parameter refers to the initial filtering flux and displays high similarities among every stirred sample. The largest value occurred when stirring was not used, while the greatest decrease in the flux was observed.

Figure 3 shows the variation of permeate flux with time when combining stirring and the US. When stirring was applied, no real difference was present in either the flux values or in the increments and indices of the fitted power functions. The steady-state values of the permeate flux were much lower for all operating conditions when stirring was not applied, but sonication produced a noticeable change. Fitted power functions show the difference between treatment types. For example, the index for 0 rpm US was

less than 60% of the index for 0 rpm no US which resulted in a minor decrease when ultrasound was used. The positive effect of ultrasound may be caused by mechanical forces or shear forces created by microstreaming and shock. The ultrasound processor applied operates at a 30 kHz frequency, where cavitation is a predominant force. Significant differences cannot be observed when both stirring, and US were used because the effect of stirring had a dominant effect on the flux behavior.

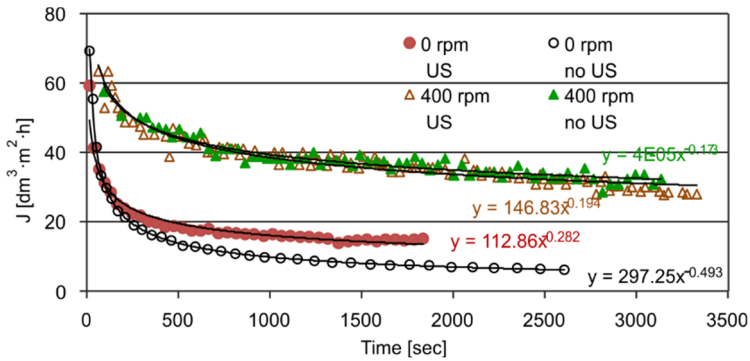


Fig. 3. Permeate flux of fermentation broth vs. time under various treatment types (US/no US means ultrasound was/was not used)

Flux data does not always give enough information about the deeper behavior of filtering parameters or mechanisms, although different types of resistances should be taken into account (Fig. 4).

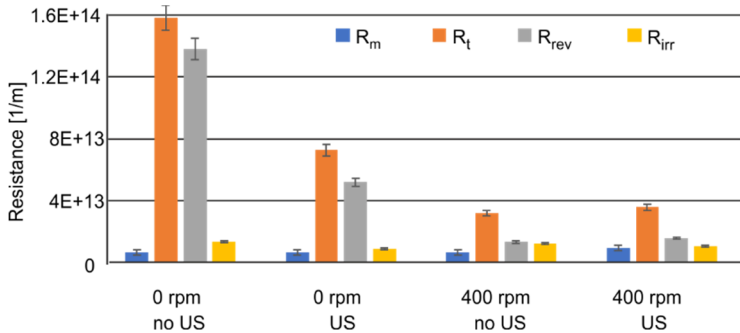


Fig. 4. Resistance values during the filtering of fermentation broth at different treatment types (R_m , R_t , R_{rev} , and R_{irr} means membrane, total, reversible and irreversible resistance; US/no US means ultrasound was/was not used)

Membrane resistances were low in all cases (Fig. 4) which implies that the selection of membrane material was appropriate because it was not the main obstacle for the separation of fermentation broth. The total resistance was significantly different from the

other types of resistances, and the total was the highest when neither stirring nor ultrasound was applied. The main contribution to the total resistance was the irreversible resistance when no stirring was applied. It was caused by the accumulated layer – that consisted of particles bigger than the pore size of the membrane (i.e., proteins, carbohydrates originated from cellulose, etc.) and the enzyme molecules themselves on the surface of the membrane, which could not be removed due to the lack of force, or present but insufficient force in the system. The irreversible resistances were smaller than expected; the layer on the surface of the membrane protected the membrane's pores from fouling and there was a quite big difference between the molecular weight of separated components (e.g., enzymes) and the cut off value, as discussed in Chapter 2. When ultrasound was applied, the resistances decreased significantly: reversible resistance decreased greatly (by 62%), while the irreversible resistance decreased by 34% compared to 0 rpm no US. This phenomenon was the consequence of ultrasound-induced cavitation and shear forces. There is a similar but more expressed tendency when stirring is applied. The value of total resistance and reversible resistances decreased significantly further (by 16 and 28%, respectively) compared to 0 rpm US but there was no significant difference between stirred and sonicated samples and samples that were only stirred but not sonicated.

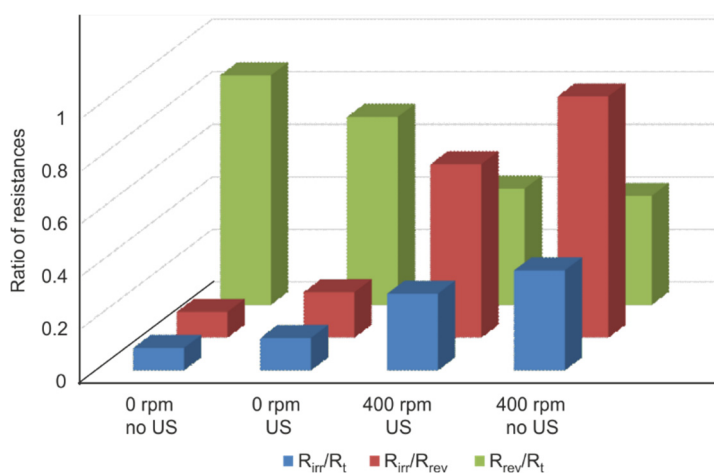


Fig. 5. Ratios of resistances (R_m , R_t , R_{rev} , and R_{irr} means membrane, total, reversible and irreversible resistance; US/no US means ultrasound was/was not used)

Ratios between different types of resistances (Fig. 5) provide useful information about the filtration mechanisms. The ratio of irreversible to total resistance without stirring was low (0.1) but stirring increased the ratio to 0.38. The ratio decreased to 0.29 when stirring and ultrasound were jointly used. This phenomenon could be explained by the following: stirring helped the particles reach the membrane pores by reducing the thickness of the gel layer above the membrane, but when ultrasound was used, cavitation assisted the particles in permeating through the membrane. An opposite tendency was

observed in the ratio of the reversible to total resistance; the ratio was the largest at samples without stirring and without sonicating, i.e., the cake above the membrane surface was the most developed. Application of stirring and/or ultrasound reduced the cake layer thickness, i.e., the value of irreversible resistance. Meanwhile, the particles had a greater chance to reach the pores, i.e., the resistance value belonging to the irreversible fouling increased. This tendency was also observed with the R_{irr}/R_{rev} ratio. The highest value occurred when stirring single-handedly was applied and smaller when both stirring, and ultrasound were applied together.

To accurately predict fouling phenomena in real solutions, Hermia's mathematical fouling models can be useful. The four main models were tested for the combinations of stirring and/or ultrasound. Figure 6 shows the matching of the experimental results to Hermia's models under various conditions.

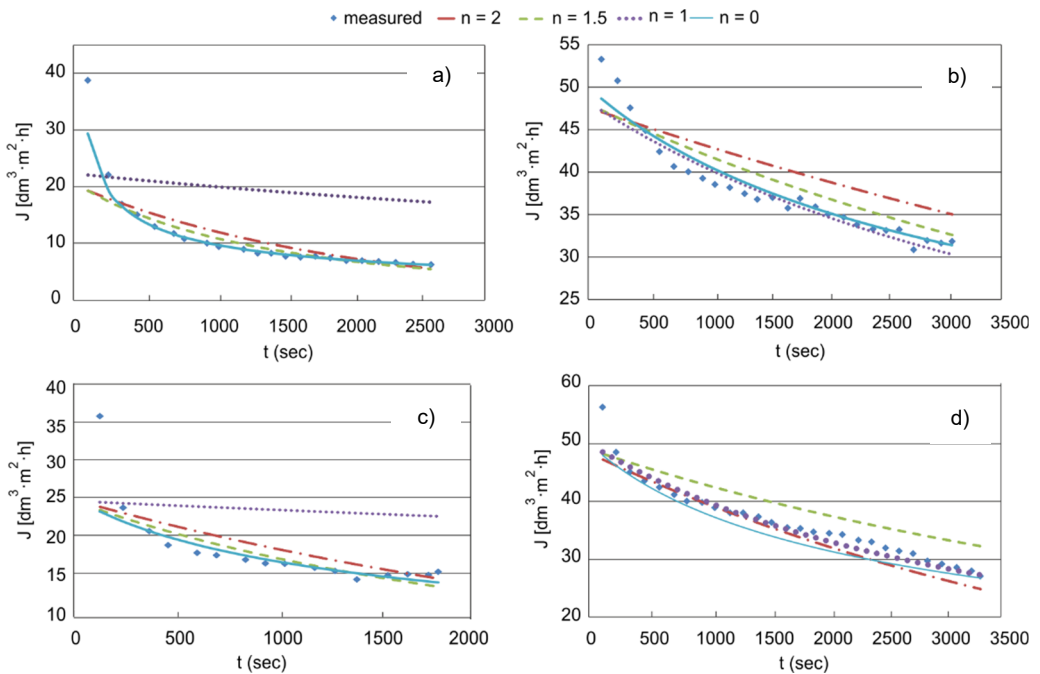


Fig. 6. Fittings of the experimental results to Hermia's models under various conditions:
 a) without stirring and sonication, b) 400 rpm stirring without sonication,
 c) sonicated but without stirring, d) stirred at 400 rpm and sonicated

Complete blocking occurs when the foulant sizes are similar to the membrane pore size, which results in reducing the number of open pores without particle deposits on the membrane surface. Intermediate blocking is similar to complete blocking to some extent, i.e., a single particle can precipitate onto other particles to form multi-layers, and it can directly block some membrane areas resulting in an increase in cake thickness.

Standard blocking is similar to adsorption, at which the particles approaching the membrane are adsorbed and deposited onto the internal pore wall thereby reducing the pore volume. Cake formation is the most severe fouling mechanism. In this process, foulants deposit on the particles that already block the pores and result in cake formation. For simplicity, the degree of model fitness (R^2) was used mainly to determine the fouling mechanisms that could explain the experimental data rationally.

Table 2

R^2 of fitted Hermia's models

Conditions	Complete pore blocking $n = 2$	Standard pore blocking $n = 1.5$	Intermediate fouling $n = 1$	Cake $n = 0$
US 0, 0 rpm	0.7494	0.8862	0.9465	0.9931
US 0, 400 rpm	0.8953	0.9153	0.932	0.9554
US 0.5, 400 rpm	0.9442	0.9599	0.9683	0.9655
US 0.5, 0 rpm	0.665	0.7189	0.7665	0.8379

For our samples, i.e., fermentation broth, it was obvious that complete and intermediate blocking, as well as gel cake formation, were fitted well to the experimental results in all cases. Table 2 shows the fitted parameter values for Hermia's models to the experimental data obtained with/without the US and with/without stirring. According to the physical meaning and the definitions of the parameters of Hermia's models (eq. 12), the values of these parameters should be higher when membrane fouling is more severe. The fitting results of the complete pore-blocking model were the smallest, and the cake formation model was the highest except when both the US and stirring were used. Regarding the molecular size distribution of the suspended and dissolved particles in broth (1–90 nm on average [21], not taking into account the negligible greater pollutants or other molecules) it was probable that most of the molecules were larger than the membrane pore (ca. 3 nm [22]), which suggests that all of the blocking mechanisms potentially occurred during the filtration process. This interpretation is consistent with the results of the measured reducing sugar concentrations discussed next.

In similar investigations, Liu et al. [1] used microfiltration to separate grape press extracts, while Simon et al. [14] for separation of dextran ($MW = 500$ kDa). Although the flux values also increased in their studies as mixing speed and US power intake increased, there were differences depending on the experimental conditions. Despite the much higher energy input/higher stirring speed of Rushton blades [1], the permeate flux increased, i.e., the efficiency value (E_{stirr}) was much lower, at least a quarter of the values found for the paddle-mixers used in the present experiments.

According to the initial and the final volume of the filtered media, the specific dissipated US power during the process ranged from 0.0255 to 0.102 W/cm³, respectively.

Stirring, despite having significantly lower energy input (P_{stirr}) than dissipated ultrasound power (P_{US}) resulted in a greater flux increase at our measurements. By increasing the mixing energy input, the efficiency factor also increased but in any case, exceeded the effect of ultrasound. The results confirm the filtration mechanisms derived from the use of the Hermia model, that is, the cake layer resistance on the membrane surface can be reduced more effectively by mixing than by the cavitation effect of US in the case of separation of high-molecular-weight molecules like proteins and/or enzymes.

Table 3

Average specific dissipated power and enhancement factors (E) for ultrasound-assisted and stirred ultrafiltration

Mode of operation	P_{stirr} [W/cm ³]	P_{US} [W/cm ³]	E
50 rpm	1.11×10^{-5}		3.6 ± 0.28
100 rpm	8.56×10^{-5}		4.9 ± 0.43
200 rpm	6.43×10^{-4}		4.39 ± 0.39
300 rpm	2.08×10^{-3}		4.3 ± 0.37
400 rpm	4.78×10^{-3}		4.94 ± 0.41
500 rpm	8.61×10^{-3}		5.12 ± 0.42
0 rpm US		4.08×10^{-2}	2.17 ± 0.29
400 rpm US	4.78×10^{-3}	4.08×10^{-2}	4.43 ± 0.35

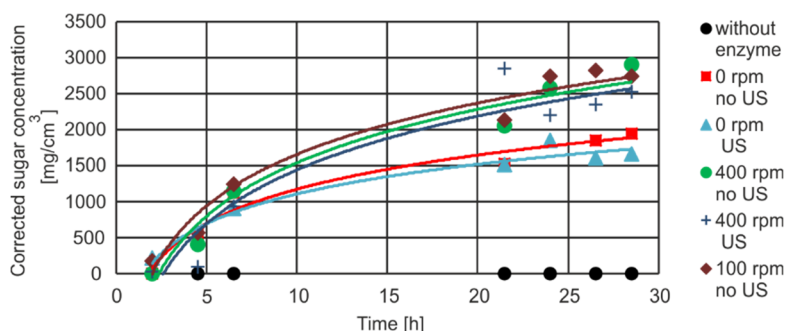


Fig. 7. Corrected reducing sugar content measured by the enzyme activity tests (US/no US means that ultrasound was/was not used)

To improve the applicability of our separation methods, i.e., to be able to reuse the separated enzyme, enzyme activity tests were carried out. The corrected reducing sugar contents measured by the enzyme activity tests are shown in Fig. 7, where the corrected sugar content refers to the deducted, residual sugar content of the samples. The initial sugar content for each curve was considered as their zero points since the residual sugar content of the samples was deducted from the current value so that only the amount of reducing sugar produced during the test should be considered.

The time dependences of the measured sugar content show that the enzymes remain active in each sample, where neither the high-speed stirring nor the sonication had a detrimental effect on the enzyme activity. Low energy sonication was also not harmful to the enzymes. A significant difference between sonicated and unsonicated samples was not found.

4. CONCLUSIONS

Ultrafiltration is an excellent separation method for enzyme recovery even from fermentation broth. The applied ultrasound (US) and/or stirring enhanced the separation efficiency and reduced the total resistance but stirring demonstrated a more beneficial effect than ultrasound on these parameters. Although there were no significant differences between the total membrane filtration resistances of combined stirred and the US or only stirred samples, the filtration mechanisms differed, i.e., Hermia's model analyses showed cake blocking mechanisms and intermediate blocking mechanisms, respectively. The result of Hermia's model was proved by the ratio of reversible and irreversible resistances. Intermediate blocking occurs when the solute molecule sizes are similar to the membrane pore size, thus some molecules can obstruct a membrane pore entrance without blocking the pore completely. Permeate flux increases with an increase of stirring speed as well as with the increase of ultrasound power. The activity of separated enzymes was satisfyingly high, i.e., neither ultrafiltration nor sonication reduced the enzyme activity.

ACKNOWLEDGMENTS

The authors are grateful for the financial support provided by the projects EFOP-3.6.2-16-2017-00010 – RING 2017 and the National Office for Research, Development, and Innovation, NKFIH/OTKA, K115691.

REFERENCES

- [1] LIU D., VOROBIEV E., SAVOIRE R., LANOISELLÉ J.L., *Comparative study of ultrasound-assisted and conventional stirred dead-end microfiltration of grape pomace extracts*, *Ultrason. Son.*, 2013, 20, 708.
- [2] SINGH S., SARMA S., AGARWAL M., GOYAL A., MOHOLKAR V.S., *Ultrasound enhanced ethanol production from *Parthenium hysterophorus*. A mechanistic investigation*, *Biores. Technol.*, 2015, 188, 287.
- [3] PRASAD S., SINGH A., JOSHI H.C., *Ethanol as an alternative fuel from agricultural, industrial and urban residues*, *Res., Cons. Rec.*, 2007, 50 (1), 1.
- [4] ŚWIERCZYŃSKA A., BOHDZIEWICZ J., *Determination of the most effective operating conditions of membrane bioreactor used to industrial wastewater treatment*, *Environ. Prot. Eng.*, 2015, 41 (1), 41.
- [5] ŚWIERCZYŃSKA A., BOHDZIEWICZ J., KAMIŃSKA G., WOJCIECHOWSKI K., *Influence of the type of membrane-forming polymer on the membrane fouling*, *Environ. Prot. Eng.*, 2016, 42 (2), 197.
- [6] GAJENDRAGADKAR C.N., GOGATE P.R., *Intensified recovery of valuable products from whey by use of ultrasound in processing steps. A review*, *Ultrason. Son.*, 2016, 32, 102.

- [7] DELGADO-POVEDANO M.M., DE CASTRO M.D.L., *A review on enzyme and ultrasound. A controversial but fruitful relationship*, Anal. Chim. Acta, 2015, 889, 1.
- [8] O'DONELL C.P., TIWARRI B.K., CULLEN P.J., *Effect of ultrasonic processing on food enzymes of industrial importance*, Trends Food Sci. Technol., 2010, 21, 385.
- [9] TUULMETS A., RAIK P., *Ultrasonic acceleration of ester hydrolyses*, Ultrason. Son., 1999, 6, 85.
- [10] VERCET A., BURGOS J., CRELIER S., LÓPEZ-BUESA P., *Inactivation of proteases and lipases by ultrasound*, Innov. Food Sci. Emerg. Technol., 2011, 2, 139.
- [11] JADHAV S.H., GOGATE P.R., *Ultrasound assisted enzymatic conversion of nonedible oil to methylesters*, Ultrason. Son., 2014, 21, 1374.
- [12] FROMET M.T., LOCKRIDGE O., MASSON P., *Resistance of butyrylcholinesterase of inactivation by ultrasound. Effect of ultrasound on catalytic activity and subunit association*, Biochim. Biophys. Acta, 1998, 1387, 53.
- [13] FIELD R., *Fundamentals of fouling*, [In:] K.-V. Peinemann, S.P. Nunes (Eds.), *Membrane Technology*, Vol. 4, *Membranes for Water Treatment*, Wiley, Weinheim 2010.
- [14] SIMON A., GONDREXON N., TAHA S., CABON J., DORANGE G., *Low frequency ultrasound to improve dead-end ultrafiltration performance*, Sep. Sci. Technol., 2000, 35, 2619.
- [15] GREEN D.W., PERRY R.H., *Perry's Chemical Engineers' Handbook*, 8th Ed., McGraw-Hill Professional, New York 2007.
- [16] MCLAREN WHITE A., SUMERFORD S.D., BRYANT E.O., LUKENS B.E., *Studies in agitation*, Ind. Eng. Chem. 1932, 24 (10), 1160.
- [17] RATONAINORO C.F., WILHELM A.M., BERLAN J., DELMAS H., *Power measurement in sonochemistry*, Ultrason. Son., 1995, 2, 543-547
- [18] MOHAMMADI T., ESMAELIFAR A., *Wastewater treatment of a vegetable oil factory by a hybrid ultrafiltration-activated carbon process*, J. Membr. Sci., 2005, 254, 129.
- [19] HERMIA J., *Constant pressure blocking filtration laws. Application to power law non-Newtonian fluids*, Trans. Inst. Chem. Eng., 1982, 60, 183.
- [20] VELA V.C.V., BLANCO S.A., GARCIA J.L., RODRIGUEZ E.B., *Analysis of membrane pore blocking models adapted to crossflow ultrafiltration in the ultrafiltration of PEG*, Chem. Eng. J., 2009, 149, 232.
- [21] CHOO K.H., LEE C.H., *Effect of anaerobic digestion broth composition on membrane permeability*, Water Sci. Technol., 1996, 34, 173.
- [22] ABELS C., CARTENSEN F., WESSLING M., *Membrane processes in biorefinery application*, J. Membr. Sci., 2013, 444, 285.